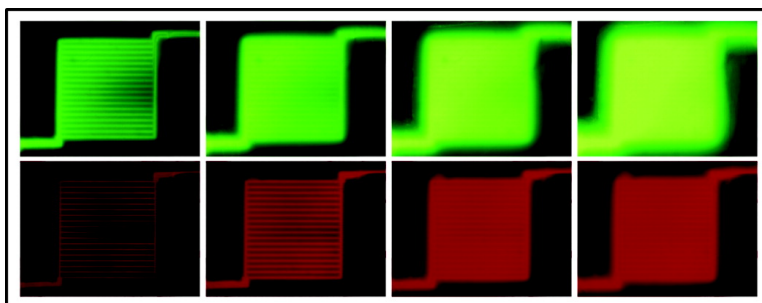


## A Microfluidic Biomaterial

Mario Cabodi, Nak Won Choi, Jason P. Gleghorn, Christopher S. D. Lee, Lawrence J. Bonassar, and Abraham D. Stroock

*J. Am. Chem. Soc.*, **2005**, 127 (40), 13788-13789 • DOI: 10.1021/ja054820t • Publication Date (Web): 15 September 2005

Downloaded from <http://pubs.acs.org> on March 25, 2009



### More About This Article

Additional resources and features associated with this article are available within the HTML version:

- Supporting Information
- Links to the 16 articles that cite this article, as of the time of this article download
- Access to high resolution figures
- Links to articles and content related to this article
- Copyright permission to reproduce figures and/or text from this article

[View the Full Text HTML](#)

## A Microfluidic Biomaterial

Mario Cabodi,<sup>†</sup> Nak Won Choi,<sup>†</sup> Jason P. Gleghorn,<sup>‡</sup> Christopher S. D. Lee,<sup>‡</sup>  
Lawrence J. Bonassar,<sup>‡,§</sup> and Abraham D. Stroock<sup>\*,†</sup>

School of Chemical and Biomolecular Engineering, Sibley School of Mechanical and Aerospace Engineering, and  
Department of Biomedical Engineering, Cornell University, Ithaca, New York 14853

Received July 19, 2005; E-mail: ads10@cornell.edu

Biomedical applications—tissue engineering, drug delivery, prosthetic implantation—demand sophisticated management of the interface between living and synthetic materials. These applications have encouraged the development of materials with biologically appropriate chemical composition, mechanical properties, rates of degradation, and micro- and macrostructure.<sup>1–3</sup> While these synthetic biomaterials have allowed for important advances in biomedical engineering,<sup>4</sup> they lack a mechanism to modulate the concentration of soluble species—metabolites, therapeutics, anti-fouling agents—within their bulk. In living tissues, this function is provided by the microvascular system, a network of convective paths that permeate their volume.<sup>5</sup> The development of microfluidics—lithographically defined channels on a 10–10<sup>3</sup> μm scale—has created an opportunity to implement this physiological strategy in synthetic biomaterials.

A successful Microfluidic Biomaterial (μFBM), a biomaterial with an embedded microfluidic network, must satisfy the conventional constraints on biomaterials as well as specific constraints for the implementation of microfluidic mass transfer. These constraints are that the material be (i) appropriate for the replication of microstructure, (ii) formable into pressure-tight fluidic structures, and (iii) highly permeable to the diffusion of small and large solutes. The second constraint requires that the material have an intrinsically low permeability to pressure-driven flow, and that it form a seal with itself and other materials (e.g., external tubing). The third characteristic is crucial as it allows for diffusive exchange of solute between the microfluidic flows and the bulk of the material. Important steps have been made toward the realization of μFBMs with the incorporation of hydrogels within microfluidic systems,<sup>6</sup> and with the fabrication of microchannels entirely within biodegradable polymers;<sup>7</sup> to our knowledge, no system has been developed that satisfies all of the above requirements.

In this communication, we report on the fabrication of a microfluidic system entirely within calcium alginate [4% (w/v)], a versatile hydrogel. We demonstrate control of mass transfer within this μFBM and illustrate that it satisfies all of the above criteria. Calcium alginate has been used extensively for tissue engineering,<sup>1,3</sup> cell culture,<sup>8</sup> and drug delivery;<sup>9</sup> its attractive intrinsic properties include low cytotoxicity, biodegradability, ability to be molded under mild conditions, mechanical stability at low solid fractions, and high permeability to diffusive mass transfer.<sup>10</sup> We employ soft lithography<sup>11</sup> to form a sealed microfluidic network in calcium alginate with pressure-tight connections to external tubing. The key steps in this process are micromolding of slabs of gel onto lithographically defined masters, and bonding of distinct slabs of

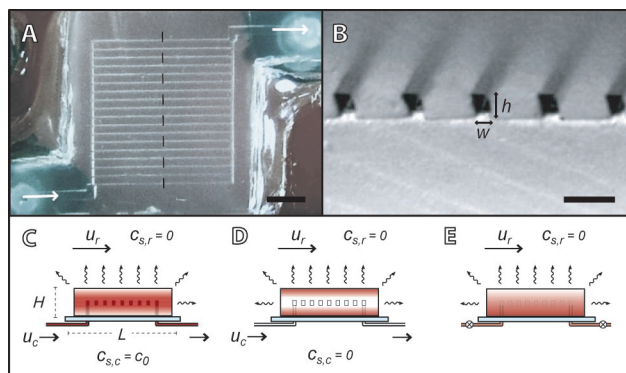


**Figure 1.** Microfluidic Biomaterial (μFBM). (A–B) Optical micrographs showing top view (A) and cross-sectional view (B) of a calcium alginate μFBM. The scale bars are 2.5 mm (A) and 500 μm (B). (C–E) Schematic diagrams of cross-section of a μFBM showing glass support, external tubing, and three modes of operation: assisted delivery of solute through the microchannels (C), assisted extraction of solute via the microchannels (D), and unassisted extraction of solute via the reservoir only (E). The shading is a schematic representation of the transient distribution of solute in the gel.  $H$  (cm) is the thickness of gel,  $L$  (cm) is the lateral dimension, and  $h$  (cm) and  $w$  (cm) are the height and width of the microchannels, respectively;  $u_r$  (cm/s) and  $u_c$  (cm/s) are the flow speeds, and  $c_{s,r}$  (mol/L) and  $c_{s,c}$  (mol/L) are the concentrations of the solute in the reservoir and the microchannels. Wavy arrows correspond to diffusive transport, and straight arrows to convective transport.

the gel to form a sealed structure. To achieve bonding, we dissolve the surfaces of the slabs with the application of sodium citrate (the citrate removes the calcium cross-links by chelating calcium),<sup>12</sup> place the dissolved surfaces in contact with one another, and re-gel the melted interfaces with the application of calcium chloride.<sup>13</sup> The micrographs in Figure 1A and 1B show a sealed microfluidic structure with channels that are 100 μm wide × 200 μm deep; we have formed sealed channels with cross-sectional dimensions as small as 25 μm × 25 μm.<sup>13</sup>

The diagrams in Figure 1C–E illustrate three modes of operation that we have used to characterize the transfer of solute in μFBMs. In all cases, we submerge the device in a stirred reservoir (200 mL;  $u_r \sim 1$  cm/s) of aqueous buffer in which the solute of interest is dilute ( $c_{s,r} \sim 0$  mol/L); this reservoir acts as a sink for the solute in the gel. We use pressure-driven flow ( $u_c \sim 0.6$  cm/s) of a distinct solution through the microchannels to either deliver ( $c_{s,c} = c_0 \neq 0$  mol/L; channels act as sources; Figure 1C) or extract ( $c_{s,c} = 0$  mol/L; channels act as sinks; Figure 1D) the solute via the microfluidic network; we refer to these modes of operation as “assisted”. Alternatively, we impose no flow through the microchannels ( $u_c = 0$  cm/s) to assess the transfer of solute with the reservoir alone (Figure 1E); we refer to this mode of operations as “unassisted”.

<sup>†</sup> School of Chemical and Biomolecular Engineering.

<sup>‡</sup> Sibley School of Mechanical and Aerospace Engineering.

<sup>§</sup> Department of Biomedical Engineering.

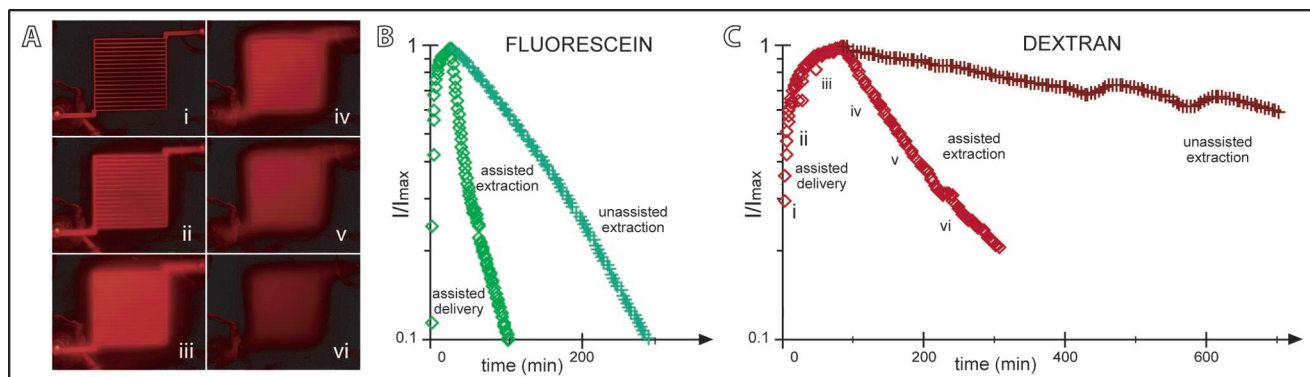


**Figure 2.** Characterization of mass transfer in a  $\mu$ FBM. (A) Fluorescence micrographs of a  $\mu$ FBM during assisted delivery (i–iii) and assisted extraction (iv–vi) of FITC–dextran. (B–C) Temporal evolution of the normalized total intensity from fluorescence images, such as those in (A), during delivery and extraction of solutes (fluorescein, MW = 376 Da; FITC–dextran, MW = 70 kDa). Diamonds represent intensities during assisted delivery and assisted extraction. Crosses represent intensities during unassisted extraction from the same initial condition (i.e., achieved by delivery via the channels) as the assisted extraction experiment. The starting time of the unassisted evacuation has been shifted to match that of the assisted extraction.  $H = 0.29$  cm,  $L = 1$  cm,  $h = 200$   $\mu$ m,  $w = 100$   $\mu$ m,  $u_r \sim 1$  cm/s,  $u_c = 0.6$  cm/s,  $c_0 = 20$   $\mu$ mol/L for fluorescein and 10  $\mu$ mol/L for FITC–dextran.

In Figure 2, we present the results of experiments in which we sequentially delivered and extracted fluorescent solutes from a  $\mu$ FBM, such as the one in Figure 1. The micrographs in Figure 2A show the transient (i, ii) and steady state (iii) distribution of solute during delivery via the microchannels (as in Figure 1C) and the transient distribution (iv–vi) during extraction via the microchannels (as in Figure 1D). In Figure 2B and C, we plot the temporal evolution of the integrated intensity from images, such as those in Figure 2A, as we performed assisted delivery, assisted extraction, and unassisted extraction of fluorescein (Figure 2B) and FITC–dextran (Figure 2C).

These experiments illustrate that (i) the  $\mu$ FBM in calcium alginate is sufficiently mechanically robust and impermeable to define distinct microfluidic paths (these devices have been tested up to positive pressures of 8 kPa and flow rates in the channels of  $u_c = 1$  cm/s); (ii) the material is permeable to the diffusion of both small and large molecules (a fit to a model of mass transfer in this geometry yields values for diffusivity in the gel that are close to those in free solution for both solutes);<sup>13</sup> (iii) a steady concentration (and flux) of solute can be achieved in the  $\mu$ FBM by continuous delivery via the channels and extraction into the bulk; and (iv) the rate of exchange of solute with the gel is increased substantially by driving flows through the microchannels, as seen by the  $\sim 3.5$ -fold difference in the time required to reach 10% of the maximum intensity between assisted and unassisted extraction (Figure 2B).

These results demonstrate the feasibility of using an embedded microfluidic system to control concentrations of soluble species within the three-dimensional volume defined by a hydrogel. The work presented here in calcium alginate is particularly relevant for the development of microfluidic scaffolds for tissue engineering, as the entire process is compatible with pre-seeding of cells within the bulk of the gel.<sup>3</sup> The realization of cell-seeded Microfluidic Biomaterials will be an important step toward the creation of physiologically accurate environments for the study and control of the development of tissues *in vitro*. More generally, microfluidic materials could be useful for the control of mass transfer in chemical contexts such as reactions mediated by immobilized catalysts or syntheses of materials in gel templates.<sup>14</sup>

**Acknowledgment.** This work was supported by the Cornell University Institute for Biotechnology and Life Science Technologies (a New York State Center for Advanced Technology), the Cornell Nanobiotechnology Center (NSF-STC, No. ECS-9876771), the Office of Naval Research, the Cornell Center for Nanoscale Science (Grant ECS 03-35765), the Cornell Center for Materials Research (NSF-MRSEC, Grant DMR-0079992), and Cornell University's College of Engineering.

**Supporting Information Available:** Details of fabrication and mass transfer (PDF) and video sequence of delivery/extraction experiment (AVI). This material is available free of charge via the Internet at <http://pubs.acs.org>.

## References

- Rowley, J. A.; Madlambayan, G.; Mooney, D. J. *Biomaterials* **1999**, *20*, 45–53.
- (a) Altman, G. H.; Horan, R. L.; Lu, H. H.; Moreau, J.; Martin, I.; Richmond, J. C.; Kaplan, D. L. *Biomaterials* **2002**, *23*, 4131–4141. (b) Boontheekul, T.; Kong, H. J.; Mooney, D. J. *Biomaterials* **2005**, *26*, 2455–2465. (c) Vozzi, G.; Flaim, C.; Ahluwalia, A.; Bhatia, S. *Biomaterials* **2003**, *24*, 2533–2540.
- Chang, S. C. N.; Rowley, J. A.; Tobias, G.; Genes, N. G.; Roy, A. K.; Mooney, D. J.; Vacanti, C. A.; Bonassar, L. J. *J. Biomed. Mater. Res.* **2001**, *55*, 503–511.
- (a) Doring, M. J.; Freese, A.; Sabel, B. A.; Saltzman, W. M.; Deutch, A.; Roth, R. H.; Langer, R. *Ann. Neurol.* **1989**, *25*, 351–356. (b) Niklason, L. E.; Gao, J.; Abbott, W. M.; Hirschi, K. K.; Houser, S.; Marini, R.; Langer, R. *Science* **1999**, *284*, 489–493.
- (a) Labarbera, M.; Vogel, S. *Am. Sci.* **1982**, *70*, 54–60. (b) Colton, C. K. *Cell Trans.* **1995**, *4*, 415–436.
- Beebe, D. J.; Moore, J. S.; Yu, Q.; Liu, R. H.; Kraft, M. L.; Jo, B. H.; Devadoss, C. *Proc. Natl. Acad. Sci. U.S.A.* **2000**, *97*, 13488–13493.
- (a) Fidkowski, C.; Kaazempur-Mofrad, M. R.; Borenstein, J.; Vacanti, J. P.; Langer, R.; Wang, Y. D. *Tissue Eng.* **2005**, *11*, 302–309. (b) King, K. R.; Wang, C. C. J.; Kaazempur-Mofrad, M. R.; Vacanti, J. P.; Borenstein, J. T. *Adv. Mater.* **2004**, *16*, 2007–2012.
- Seifert, D. B.; Phillips, J. A. *Biotechnol. Prog.* **1997**, *13*, 562–568.
- Gombotz, W. R.; Wee, S. F. *Adv. Drug Delivery Rev.* **1998**, *31*, 267–285.
- Li, R. H.; Altreuter, D. H.; Gentile, F. T. *Biotechnol. Bioeng.* **1996**, *50*, 365–373.
- McDonald, J. C.; Chabinyc, M. L.; Metallo, S. J.; Anderson, J. R.; Stroock, A. D.; Whitesides, G. M. *Anal. Chem.* **2002**, *74*, 1537–1545.
- Masuda, K.; Sah, R. L.; Hejna, M. J.; Thonar, E. J.-M. A. *J. Ortho. Res.* **2003**, *21*, 139–148.
- See Supporting Information for details.
- (a) Gundiah, G.; Mukhopadhyay, S.; Tumkurkar, U. G.; Govindaraj, A.; Maitra, U.; Rao, C. N. R. *J. Mater. Chem.* **2003**, *13*, 2118–2122. (b) Guisan, J. M.; Bastida, A.; Cuesta, C.; Fernandezlafuente, R.; Rosell, C. M. *Biotechnol. Bioeng.* **1991**, *38*, 1144–1152.

JA054820T